

## A New Material Model for 2D FE Analysis of Adhesively Bonded Composite Joints

Libin ZHAO<sup>1</sup>, Yana WANG<sup>1</sup>, TianLiang QIN<sup>1</sup>, Jianyu ZHANG<sup>2\*</sup>

<sup>1</sup> School of Astronautics, Beihang University, Beijing 100191, P.R. China

<sup>2</sup> Institute of Solid Mechanics, Beihang University, Beijing 100191, P.R. China

**crossref** <http://dx.doi.org/10.5755/j01.ms.20.4.5960>

Received 18 December 2013; accepted 11 October 2014

Effective and convenient stress analysis techniques play important roles in the analysis and design of adhesively bonded composite joints. A new material model is presented at the level of composite ply according to the orthotropic elastic mechanics theory and plane strain assumption. The model proposed has the potential to reserve nature properties of laminates with ply-to-ply modeling. The equivalent engineering constants in the model are obtained only by the material properties of unidirectional composites. Based on commercial FE software ABAQUS, a 2D FE model of a single-lap adhesively bonded joint was established conveniently by using the new model without complex modeling process and much professional knowledge. Stress distributions in adhesive were compared with the numerical results by Tsai and Morton and interlaminar stresses between adhesive and adherents were compared with the results from a detailed 3D FE analysis. Good agreements in both cases verify the validity of the proposed model.

*Keywords:* composite bonded joints, analytical model, mechanical properties, finite element analysis (FEA).

### 1. INTRODUCTION

Adhesively bonded composite joints are effective connections between composite parts. They have attracted significant attentions in aerospace industries [1] due to remarkable advantages, such as easy integrated manufacture, low assembly weight, minimal sources of stress concentration, smooth load transfer and superior fatigue and damage tolerance performances. However, the joints are discontinuities of structures and thus potential weakness under load conditions. Generally, three failure modes including failure within composite adherents, failure within the adhesive and interface debonding between the adhesive and composite adherents, may take place in adhesively bonded joints. Therefore, an accurate and convenient FE analysis to illustrate the stress distribution in the composite adherents and adhesive is necessary for further prediction of strength and failure.

In order to obtain the information of stress and strain distributions of adhesively bonded joints, many analytical methods have been developed [2–7]. However, analytical methods show limitations such as some assumptions or simplification, and thus are only utilized in specific cases with simple configuration. With the development of finite element (FE) techniques and computers, the FE method has become the most significant approach of stress analysis due to its revolutionary simulation capability for composite structures with arbitrary geometry and stacking sequences under complicated loading conditions. Many FE models have been presented for composite adhesively bonded joints [8–12], which can be split into two general categories: 2D models and 3D models. The 2D models were developed before 3D models due to the computing capability limitations of early computers. The 2D models

were usually established based on assumptions of plane strain or plane stress. Wooley and Carver [13] first used plane stress element to construct the 2D FE model of single-lap bonded joint, in which the adhesive layer was modelled with two rows of elements to obtain the stress variation across the adhesive thickness, and linear analysis were performed based on the FE model. After the pioneering research of Wooley and Carver, many similar linear finite element analyses with several improvements, such as refined meshes for the adhesive [14] and introducing adhesive deformation [15], were conducted. 2D FE models with plane strain element were also developed. Adams and Peppiatt [16] simulated a single-lap joint with plane strain triangular elements. In addition, nonlinear behaviours were gradually included in analyses. Cooper and Sawyerb [17] first developed 2D FE models accounting for geometric nonlinearities. Adams [18] performed a nonlinear analysis including the material and geometric nonlinearities for a FE model of the adhesively bonded joint using triangular and quadrangular plane strain elements. With the 2D FE analysis incorporating non-linearity of both the adherent and adhesive, Adams and his co-workers [19] studied the joints end effects to understand the spew fillets and adherent tapering of the adhesively single-lap joint. Moreover, some researchers developed special elements to model the behaviour of the adhesive [20–28]. Barker and Hatt [20] published the first works on the special elements with a four-node two-dimensional element. Carpenter and Barsoum [23] proposed specific elements with some assumptions used in several analytical studies, which could be used in 2D plane stress or plane strain elements.

With the rapid developments in computing capacity of computer, 3D FE models, which can characterize the 3D nature of structural stresses [29], attract more attentions in adhesively bonded joints. The 3D FE models are not only

\*Corresponding author. Tel.: +86-10-82338663; fax: +86-10-82339228.  
E-mail address: [jy Zhang@buaa.edu.cn](mailto:jy Zhang@buaa.edu.cn) (J. Y. Zhang)

suitable for simulation of complex structural configuration [30–38] but also effective to obtain more accurate stress distribution and reveal the transverse stress effects [29, 39]. However, the modelling process is perplexing and exhaustive at time cost to those who are short of professional knowledge. Moreover, the computational cost of 3D models is terrifically high, especially for fine mesh scheme, iterative repetition computation, or large scale problems, etc. In contrast, the 2D FE model is time-saving and easy to operate. With the improvement of composite material technologies, more and more complex joint structures, such as the out-of-plane joints, challenge the current FE modelling method, as the modelling and computing costs of such complex structures are quite high. Therefore a simple and accurate 2D FE modelling method is still needed in practical engineering applications due to its low computing cost, especially for fast design and effective parametric investigation.

In 2D FE models of composite adhesively bonded joints, the material properties of the isotropic adhesive layer can be easily defined in plane elements. As for the composite materials, however, the material properties in the plane stress or strain element, which is often oblique referred to fiber direction of lamina, are difficult to set, except for special cases that the fiber is along with or vertical to the element plane [40]. To overcome this knottiness, most of the proposed 2D models used effective material properties of the whole laminate calculated by the Classical Laminated Theory. Although they retained some natures of the composite laminates to a certain extent, they hardly described the layer stress and interlaminar stress accurately since they regarded the laminate as an orthotropic body. To solve this problem, in this paper, a new material model is presented to characterize the plane element at the level of composite ply according to the orthotropic elastic mechanics theory. The model proposed offers an easy way to establish a 2D ply-to-ply FE model for composite structures with physically based material properties of unidirectional lamina, which is competitive in engineering since it brings not only accurate layer and interlaminar stress solutions but also low time and cost consuming. To verify the model, a single-lap adhesively-bonded joint used by Tsai and Morton [41] was adopted here as a benchmark. A 2D FE model was constructed using the material model proposed with the software ABAQUS. The stress distribution in the adhesive was verified by the results obtained by Tsai and Morton. Besides, the interlaminar stress distribution at the interface between the adhesive and adherents was validated by the stress analysis obtained from a 3D FE model under the guidance from Diaz et al. [42].

## 2. MODEL DESCRIPTION

Consider an arbitrary unidirectional fiber reinforced composite ply with principal axes 1(longitudinal, fiber direction), 2 (transverse direction) and 3 (interlaminar direction), as shown in Fig. 1, a.

According to the orthotropic elastic mechanics theory, the ply can be assumed as transversely isotropic materials in the principal coordinate system  $O-123$  and its constitute relationship is written as:

$$\begin{Bmatrix} \varepsilon_1 \\ \varepsilon_2 \\ \varepsilon_3 \\ \gamma_{23} \\ \gamma_{31} \\ \gamma_{12} \end{Bmatrix} = \begin{bmatrix} S_{11} & S_{12} & S_{12} & 0 & 0 & 0 \\ S_{21} & S_{22} & S_{23} & 0 & 0 & 0 \\ S_{21} & S_{32} & S_{22} & 0 & 0 & 0 \\ 0 & 0 & 0 & 2(S_{22} - S_{23}) & 0 & 0 \\ 0 & 0 & 0 & 0 & S_{66} & 0 \\ 0 & 0 & 0 & 0 & 0 & S_{66} \end{bmatrix} \begin{Bmatrix} \sigma_1 \\ \sigma_2 \\ \sigma_3 \\ \tau_{23} \\ \tau_{31} \\ \tau_{12} \end{Bmatrix}, \quad (1)$$

where  $S_{ij}$  are the elements of the compliance matrix, and can be expressed by the engineering constants  $E_1, E_2, \nu_{12}, \nu_{23}$  and  $G_{12}$ .

The equation (1) can be simplified as matrix form:

$$\{\varepsilon\} = [\mathbf{S}]\{\sigma\}. \quad (2)$$

The strain-stress relationship of the ply referred to an arbitrary Cartesian coordinates  $O-XYZ$  can be rewritten as:

$$\{\bar{\varepsilon}\} = [\bar{\mathbf{S}}]\{\bar{\sigma}\}, \quad (3)$$

where  $\{\bar{\varepsilon}\}$  and  $\{\bar{\sigma}\}$  are expressed as:

$$\{\bar{\varepsilon}\} = \{\varepsilon_x \quad \varepsilon_y \quad \varepsilon_z \quad \gamma_{yz} \quad \gamma_{zx} \quad \gamma_{xy}\}^T, \quad (4)$$

$$\{\bar{\sigma}\} = \{\sigma_x \quad \sigma_y \quad \sigma_z \quad \sigma_{yz} \quad \sigma_{zx} \quad \sigma_{xy}\}^T,$$

where  $\{\bar{\varepsilon}\}$  and  $\{\bar{\sigma}\}$  are off-axis strain and stress vectors corresponding to the coordinate system  $O-XYZ$ .  $[\bar{\mathbf{S}}]$  is the related off-axis compliance matrix which can be derived from compliance matrix  $[\mathbf{S}]$ , stress transformation matrix  $[\mathbf{T}_\sigma]$  and strain transformation matrix  $[\mathbf{T}_\varepsilon]$ .

$$[\bar{\mathbf{S}}] = [\mathbf{T}_\varepsilon]^{-1}[\mathbf{S}][\mathbf{T}_\sigma], \quad (5)$$

where  $[\mathbf{T}_\sigma]$  and  $[\mathbf{T}_\varepsilon]$  are expressed as:

$$[\mathbf{T}_\sigma] = \begin{bmatrix} m^2 & n^2 & 0 & 0 & 0 & 2mn \\ n^2 & m^2 & 0 & 0 & 0 & -2mn \\ 0 & 0 & 1 & 0 & 0 & 0 \\ 0 & 0 & 0 & m & -n & 0 \\ 0 & 0 & 0 & n & m & 0 \\ -mn & mn & 0 & 0 & 0 & m^2 - n^2 \end{bmatrix}, \quad (6)$$

$$[\mathbf{T}_\varepsilon] = \begin{bmatrix} m^2 & n^2 & 0 & 0 & 0 & mn \\ n^2 & m^2 & 0 & 0 & 0 & -mn \\ 0 & 0 & 1 & 0 & 0 & 0 \\ 0 & 0 & 0 & m & -n & 0 \\ 0 & 0 & 0 & n & m & 0 \\ -2mn & 2mn & 0 & 0 & 0 & m^2 - n^2 \end{bmatrix},$$

where  $m = \cos\theta, n = \sin\theta$  are directional cosines referred to the fiber direction, which is shown in Fig. 1, a.

Equation (3) can be transposed as:

$$\{\bar{\sigma}\} = [\bar{\mathbf{S}}]^{-1}\{\bar{\varepsilon}\} = [\bar{\mathbf{C}}]\{\bar{\varepsilon}\}. \quad (7)$$

Referred to the coordinate system  $O-XYZ$ , it can be seen from Fig. 1, a, that the ply is an orthotropic solid body with one symmetric plane  $X-O-Y$ , thus the off-axis stiffness matrix  $[\bar{\mathbf{C}}]$  has the following form [43]:

$$[\bar{\mathbf{C}}] = \begin{bmatrix} \bar{C}_{11} & \bar{C}_{12} & \bar{C}_{13} & 0 & 0 & \bar{C}_{16} \\ \bar{C}_{21} & \bar{C}_{22} & \bar{C}_{23} & 0 & 0 & \bar{C}_{26} \\ \bar{C}_{31} & \bar{C}_{32} & \bar{C}_{33} & 0 & 0 & \bar{C}_{36} \\ 0 & 0 & 0 & \bar{C}_{44} & \bar{C}_{45} & 0 \\ 0 & 0 & 0 & \bar{C}_{54} & \bar{C}_{55} & 0 \\ \bar{C}_{61} & \bar{C}_{62} & \bar{C}_{63} & 0 & 0 & \bar{C}_{66} \end{bmatrix}. \quad (8)$$

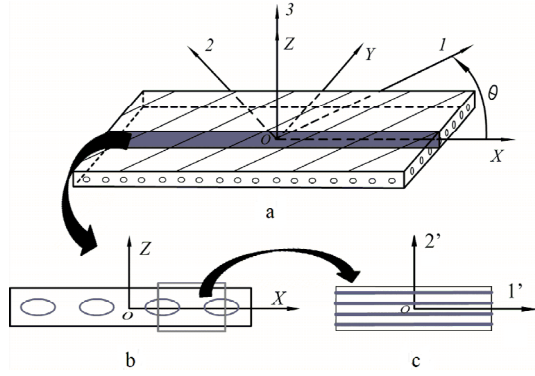


**Fig. 1.** Sketch map of the new material model: a – composite ply with angle; b – middle plane; c – equivalent ply

As the composite laminates are always symmetrical balanced, in which case the bending-twist coupling of ply is ignored. Moreover, as adhesively bonded joints are commonly wide compared with its thickness, and the plane strain assumption can be adopted in the stress analysis of the joints. Thus in the plane  $X$ - $O$ - $Z$  we have:

$$\begin{aligned} \varepsilon_y &= 0 \\ \gamma_{yz} &= 0 \\ \gamma_{xy} &= 0 \end{aligned} \quad (9)$$

Substitute equation (9) into equation (7). Thus the constitutive equation in  $X$ - $O$ - $Z$  plane, as shown in Fig. 1, b, could be derived as:

$$\begin{Bmatrix} \sigma_x \\ \sigma_z \\ \tau_{xz} \end{Bmatrix} = \begin{bmatrix} \bar{C}_{11} & \bar{C}_{13} & 0 \\ \bar{C}_{31} & \bar{C}_{33} & 0 \\ 0 & 0 & \bar{C}_{55} \end{bmatrix} \begin{Bmatrix} \varepsilon_x \\ \varepsilon_z \\ \gamma_{xz} \end{Bmatrix} \quad (10)$$

The strain-stress relationship can be transposed as:

$$\begin{Bmatrix} \varepsilon_x \\ \varepsilon_z \\ \gamma_{xz} \end{Bmatrix} = \begin{bmatrix} \bar{s}'_{11} & \bar{s}'_{12} & 0 \\ \bar{s}'_{12} & \bar{s}'_{22} & 0 \\ 0 & 0 & \bar{s}'_{33} \end{bmatrix} \begin{Bmatrix} \sigma_x \\ \sigma_z \\ \tau_{xz} \end{Bmatrix}, \quad (11)$$

where  $\bar{s}'_{ij}$  are compliance coefficients with respect to the  $X$ - $O$ - $Z$  plane.

There are two forms of data input in existed FE commercial code for composite structures. One is to set engineering constants of unidirectional composites combined with information of laminates, including stacking sequences, the number of lamina, each lamina thickness etc. The other regards the composite laminate as an orthotropic solid body and thus input a  $6 \times 6$  stiffness matrix calculated by Classical Laminate Theory.

In this paper, an equivalent lamina or plane stress element (see Fig. 1, c) is introduced to characterize the material properties in plane  $X$ - $O$ - $Z$ . This provides a means to input data into the commercial software using the first form mentioned above. The introduced equivalent lamina or plane stress element has the same constitutive relationship as equation (11). Assume the principal axes of the equivalent lamina or element are  $1'$  (longitudinal, fiber direction) and  $2'$  (transverse direction). The corresponding engineering constants are denoted by  $E_{1'}$ ,  $E_{2'}$ ,  $\nu_{12'}$ ,  $G_{12'}$ . Thus, the strain-stress relationship of the equivalent lamina is:

$$\begin{Bmatrix} \varepsilon_{1'} \\ \varepsilon_{2'} \\ \gamma_{12'} \end{Bmatrix} = \begin{bmatrix} 1/E_{1'} & -\nu_{12'}/E_{1'} & 0 \\ -\nu_{12'}/E_{1'} & 1/E_{2'} & 0 \\ 0 & 0 & 1/G_{12'} \end{bmatrix} \begin{Bmatrix} \sigma_{1'} \\ \sigma_{2'} \\ \tau_{12'} \end{Bmatrix}. \quad (12)$$

Therefore, new engineering constants could be derived as follows:

$$\begin{aligned} E_{1'} &= 1/\bar{s}'_{11} \\ E_{2'} &= 1/\bar{s}'_{22} \\ \nu_{12'} &= -\bar{s}'_{12}/\bar{s}'_{11} \\ G_{12'} &= 1/\bar{s}'_{33} \end{aligned} \quad (13)$$

Equation (13) gives the new material model established at the level of physical composite ply with arbitrary angle, which could be obtained by the compliance coefficients in equation (11). Thus 2D models could be established with the FE commercial code to simulate the adhesively bonded composite joints.

### 3. NUMERICAL VERIFICATION

A single-lap adhesive-bonded joint used by Tsai and Morton [41] was adopted here as a benchmark. The joint was also utilized by Diaz et al. [42] to study the modeling techniques for 3D accuracy stress and strain responses.

The joint configuration, dimensions and boundary condition are shown in Fig. 2, a. A uniform tensile load  $P = 4448$  N [41] was applied at the right end of the upper adherent along the longitudinal direction of the joint. The left end of the lower composite adherent was totally fixed with a length of 20 mm, while the right end of the upper adherent was only restricted in the transverse and normal direction. The dimensions of the joint are listed in Table 1. The adherents were made of graphite/epoxy (XAS/914C) unidirectional composite materials with a lay-up of  $[0/45/45/0]_s$ , and the adhesive layer was made of epoxy adhesive (Hexcel Redux 308A). The material properties of the composite adherents and the adhesive, among which the latter is commonly regarded as isotropic elastic material, are listed in Table 2. The interlaminar properties of composite lamina were given by transverse isotropic assumption or engineering experiences:  $E_2 = E_3$ ,  $\nu_{12} = \nu_{13} = \nu_{23}$ ,  $G_{12} = G_{13} = G_{23}$ . According to the section 2, the equivalent engineering constants in the joint symmetrical plane for plies with different angles are listed in Table 3.

**Table 1.** Dimensions of the joint

$L$ , mm	$2c$ , mm	$B$ , mm	$t$ , mm	$t_a$ , mm
101.6	25.4	25.4	2.0	0.13

**Table 2.** Material properties of composite adherent and adhesive

Properties	$E_1$ , GPa	$E_2$ , GPa	$G_{12}$ , GPa	$\nu_{12}$
Adherent	138.0	9.4	6.7	0.32
Adhesive	$E=3.0$ GPa		1.15	0.31

**Table 3.** Equivalent engineering constants of different plies

Ply orientation	$E_{1'}$ , GPa	$E_{2'}$ , GPa	$G_{12'}$ , GPa	$\nu_{12'}$
$0^\circ$	138.97	10.47	6.70	0.43
$\pm 45^\circ$	45.32	10.27	5.13	0.38

A 2D FE model of the joint employing the new material model was established here. The zone near the adhesive was partially shown in Fig. 2, b. During the 2D FE modeling, the material properties of composite plies with different angles had been assigned to corresponding ply section respectively. CPS4 (4-node bilinear plane stress quadrilateral) element was adopted. Besides, to perform the geometric nonlinear analysis, the 'Nlgeom' was set at the 'on' state in ABAQUS. Different mesh densities were defined in different regions of the joint. Refined meshes were used in the overlap region, especially at the two ends of the adhesive, where the stress field suffered great stress gradient. The meshes in the other region were relatively coarse. Trapezoidal meshes were used in transition part of the adherents adjacent to the two ends of adhesive to ensure smooth transitions between the overlapped region and un-overlapped region. The adhesive layer was divided into 6 elements through thickness.

Meanwhile, a 3D FE model with C3D8 solid elements was established according to 3D FE modeling techniques of Diaz et al. [42], as depicted in Fig. 2, c. The same mesh scheme as that of the 2D FE model was used in the 3D FE model. Also, the geometric nonlinear was taken into account.

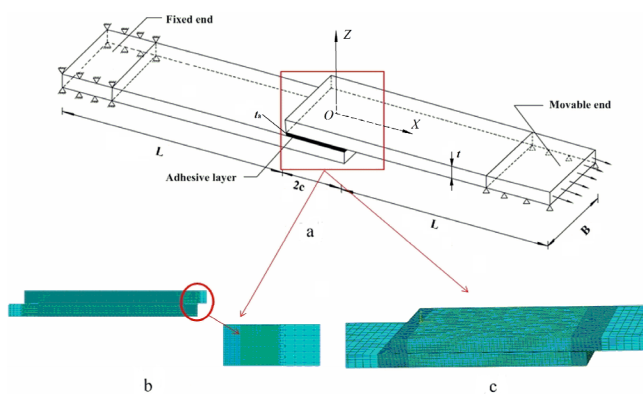


**Fig. 2.** Configuration and FE models of single-lap adhesively bonded joint: a – configuration, load and boundary conditions; b – 2D FE model; c – 3D FE model

For the single-lap adhesively bonded joint, the peel stress and shear stress in the adhesive, which always lead to adhesive failure, play an important role in estimating joint strength. Therefore, the accurate stress analysis in the adhesive is significant. Through the finite element analysis, the shear and peel stress distributions in the middle of adhesive layer were obtained and compared with the results from Tsai and Morton [41]. Besides, the interlaminar stress between adhesive and upper adherent was verified by the results stemming from the 3D FE analysis. All the stress results were normalized by dividing the laminate average stress ( $p = P/Bt = 87.56$  MPa). In addition, only the stress distributions of the right half part of the bonding line was given by Tsai and Morton, since they considered symmetrical shear and peel stress distribution within the adhesive.

Fig. 3, a, gives the normalized shear stress distribution within the middle of adhesive obtained from the 2D FE model and that from analysis result by Tsai and Morton [41]. It can be seen that shear stresses within adhesive have a symmetrical but strong non-uniform distribution. In

addition, good agreements between two curves can be observed except for the most outside points. Tsai and Morton's results show the shear stress at the end of the adhesive reaches the peak value. However, from the 2D FE model, it can be found that the maximum shear stress appears adjacent to the end of the overlap while the shear stress at the end of the overlap is relatively low. Due to the shear stress reciprocal theorem, it is clear the results from the 2D FE model are reasonable. Moreover, the maximum shear stress near the adhesive end will significantly limit the joint load bearing capability. Fig. 3, b, gives the peel stress results within the adhesive from the 2D FE model and Tsai and Morton [41]. The peel stress distribution within the adhesive is also symmetrical but strong non-uniform along the bond line. However, the maximum value of the peel stress occurs at the end of the adhesive. The peel stress decreases sharply from the end toward the inside. In most part of the interface, the peel stress is almost zero. The high peel stress at the end increases the danger of the joint. Besides, the results from the 2D FE model and Tsai and Morton are in good agreements.

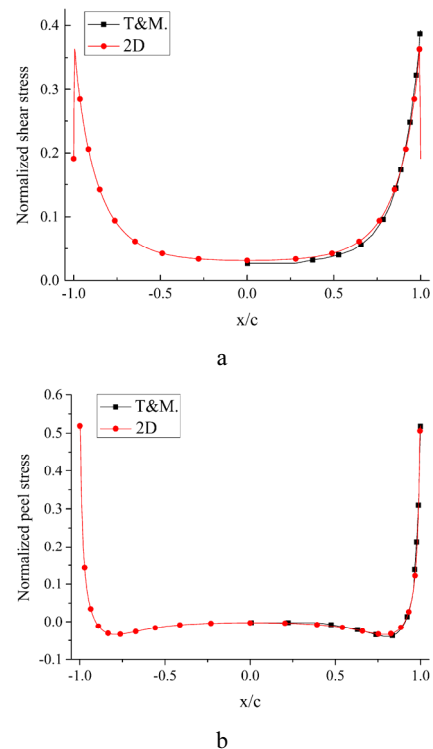


**Fig. 3.** Stress distributions in the middle of adhesive layer obtained from 2D FE model and Tsai and Morton: a – normalized shear stress; b – normalized peel stress

For single-lap adhesively bonded joint, the composite adherent near the overlap part is another critical position, in which delamination often occurs, due to low interlaminar strength of composite materials. Fig. 4, a, and Fig. 4, b, illustrate the normalized interlaminar shear and peel stress distribution at the interface between the adhesive and upper adherent obtained from the 2D and 3D FE models, respectively. The results from the 3D FE analysis were taken from the transverse middle plane of the joint. Obviously, the numerical results from 2D and 3D FE analyses are in good consistent. In addition, unlike symmetrical stress distribution in the middle of adhesive,

the shear stress within the interface presents different distribution rules. The shear stress at the left end of the overlap is negative. As the distance away from the free end increases, the shear stress sharply increases followed by a gradually decrease up to a small positive value, which possesses most region of the overlap. Then the shear stress gradually increases near the right free end. After a small wave, the shear stress steeply enhances to the maximum value at the right end of the overlap. The maximum shear stress provided by the 2D FE model is 4.61 % lower than the one obtained from the 3D FE model.

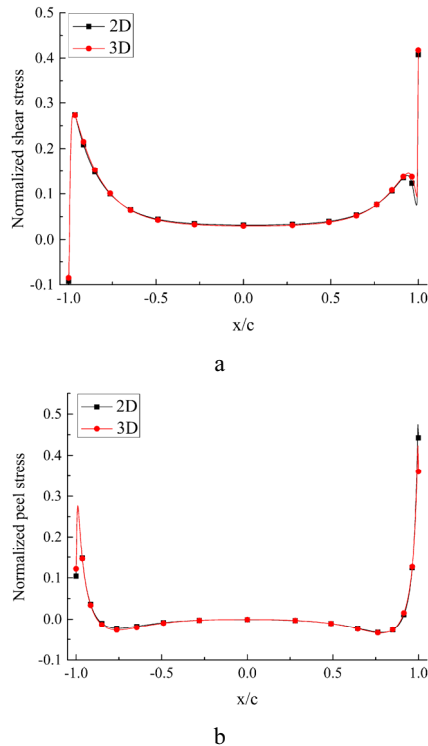


**Fig. 4.** Interlaminar stress between the adhesive and upper adherent obtained from the 2D and 3D FE models: a – normalized shear stress; b – normalized peel stress

As illustrated in Fig. 4, b, the peel stress is comparatively high at the end of the composite adherent, but it drops quickly in a small distance apart from the ends. In most region of the overlap the peel stress is approximately zero. The maximum peel stress, which occurs near the right end of the adhesive, provided by the 2D FE model is 12.04 % higher than that obtained from the 3D FE model. It is inclined to induce delamination due to the low interlaminar strength. As there is severe stress concentration at the end of the overlaps, the result of linear elastic FE models can only be used to describe the stress distribution qualitatively. The FE model with nonlinear material properties is required to reveal the accurate stresses at the end of the overlaps [6].

In general, the 2D FE model and 3D FE model have provided almost the same stress results for single-lap adhesively bonded joint. Both of them give the reasonable interlaminar stress between the adhesive and upper adherent as well as indicate the potential critical region in the single-lap adhesively bonded joint. However, the 2D model based on the new material model proposed in this paper saves much modeling time and computational cost.

The 2D FE analysis was completed within 7 seconds while the 3D FE analysis cost the computing time of 3 hours and 27 minutes, following which the 2D FE model is a good choice on account of its high efficiency and accuracy.

#### 4. CONCLUSIONS

A new material model at the level of composite ply, which could reserve the nature properties of composite laminates through ply-to-ply modelling method, is proposed based on the orthotropic elastic theory and plane strain assumption. The equivalent engineering constants of each ply with different angles are presented by given material properties of unidirectional lamina. The 2D FE model of single-lap adhesively bonded joint was established using plane stress element with equivalent engineering constants. To verify the validity of the new material model, the shear and peel stress distribution in the middle of adhesive layer obtained from the 2D FE analysis using the new material model are compared with the results from Tsai and Morton. Meanwhile, the interlaminar stress distribution at the interface between the adhesive and upper adherent obtained from the 2D FE and 3D FE analyses are compared. For the above two cases, the results from the 2D FE model are all in good agreements with the counterparts stemming from Tsai and Morton or 3D FE model, which gives evidence of the validity of the new material model. On account of the high efficiency and convenience of the 2D FE model, the material model proposed here is perfectly useful for industrial usage, especially for a fast design and effective parametric investigations.

#### Acknowledgments

The research work is supported by the National Science Foundation of China (10902004, 11372020).

#### REFERENCES

1. Pandey, P.-C., Shankaragouda, H., Singh, A.-K. Non-linear Analysis of Adhesively Bonded Lap Joints Considering Viscoplasticity in Adhesives *Computers & Structure* 70 1999: pp. 387–413.
2. Hart-Smith, L.-J. Adhesive-bonded Single-lap Joints. Report CR 112236, Douglas Aircraft Co., USA, 1973.
3. Hart-Smith, L.-J., Adhesive-bonded Double-lap Joints. Report CR 112235, Douglas Aircraft Co., USA, 1973.
4. Delale, F., Erdogan, F., Aydinoglu, M.-N. Stresses in Adhesively Bonded Joints a Closed-form Solution *Journal of Composite Materials* 15 1981: pp. 249–271.
5. Pickett, A.-K., Hollaway, L. The Analysis of Elastic-plastic Adhesive Stress in Bonded Lap Joints in FRP Structures *Computers & Structure* 4 1985: pp. 135–160.
6. Mortensen, F., Thomsen, O.-T. Analysis of Adhesive Bonded Joints: a Unified Approach *Composites Science and Technology* 62 2002: pp. 1011–1031.
7. Zou, G.-P., Shahin, K., Taheri, F. An Analytical Solution for the Analysis of Symmetric Composite Adhesively Bonded Joints, *Composite & Structure* 65 (3–4) 2004: pp. 499–451.
8. Tsai, M. Y., Morton, J., Matthews, F.-L. Experimental and Numerical Studies of a Laminated Composite Single-lap Adhesive Joint *Journal of Composite Materials* 29 1995: pp. 1254–1275.

9. **Li, G., Lee Sullivan, P.** Finite Element and Experimental Studies on Single-lap Balanced Joints in Tension *International Journal of Adhesion and Adhesive* 21 2001: pp. 211–220.
10. **Richardson, G., Crocombe, A.-D., Smith, P.-A.** A Comparison of Two- and Three-dimensional Finite Element Analyses of Adhesive Joints *International Journal of Adhesion and Adhesive* 13 1993: pp. 193–200.
11. **Castagnetti, D., Dragoni, E.** Failure Analysis of Bonded T-peel Joints: Efficient Modeling by Standard Finite Elements with Experimental Validation *International Journal of Adhesion and Adhesive* 30 2010: pp. 306–312.
12. **Feih, S., Shercliff, H.-R.** Composite Failure Prediction of Single-L Joint Structures Under Bending *Composites: Part A* 36 2005: pp. 381–395.  
<http://dx.doi.org/10.1016/j.compositesa.2004.06.021>
13. **Wooley, G. R., Carver, D. R.** Stress Concentration Factors for Bonded Lap Joints *Journal of Aircraft* 8 (10) 1971: pp. 817–820.
14. **Guess, T.R., Allred, R. E., Gerstle, F. P.** Comparison of Lap Shear Test Specimens *Journal of Testing and Evaluation* 5 (2) 1977: pp. 84–93.
15. **Harrison, N. L., Harrison, W. J.** The Stresses in An Adhesive Layer *International Journal of Adhesion and Adhesives* 3 (3) 1972: pp. 195–212.
16. **Adams, R. D., Peppiatt, N. A.** Stress Analysis of Adhesively Bonded Lap Joints *Journal of Strain Analysis for Engineering Design* 9 1974: pp. 185–196.  
<http://dx.doi.org/10.1243/03093247V093185>
17. **Cooper, P. A., Sawyer J. W.** A Critical Examination of Stresses in an Elastic Single Lap Joint. NASA, 1979.
18. **Harris, J. A., Adams, R. D.** Strength Prediction of Bonded Single Lap Joints by Nonlinear Finite Element Methods , *International Journal of Adhesion and Adhesives* 4 1984: pp. 65–78.  
[http://dx.doi.org/10.1016/0143-7496\(84\)90103-9](http://dx.doi.org/10.1016/0143-7496(84)90103-9)
19. **Adams, R. D., Wake, W. C.** The Nature and Magnitude of Stresses in Adhesive Joints *Structure Adhesive Joints in Engineering* Amsterdam: Elsevier Applied Science Publisher 2 1984: pp. 14–114.  
[http://dx.doi.org/10.1007/978-94-009-5616-2\\_2](http://dx.doi.org/10.1007/978-94-009-5616-2_2)
20. **Barker. R. M., Hatt, F.** Analysis of Bonded Joint in Vehicular Structure *AIAA Journal* 11 (12) 1973: pp. 1650–1654.
21. **Carpenter, W. C.** Finite Element Analysis of Bonded Connections *International Journal for Numerical Methods in Engineering* 6 (3) 1973: pp. 450–451.  
<http://dx.doi.org/10.1002/nme.1620060318>
22. **Carpenter, W. C.** Stress in Bonded Connections Using Finite Elements *International Journal for Numerical Methods in Engineering* 15 1980: pp. 1659–1680.
23. **Carpenter, W. C.** Two Finite Elements for Modeling the Adhesive in Bonded Configurations *Journal of Adhesion* 30 1989: pp. 25–46.
24. **Rao, B. N., Rao, V. K.** Analysis of Composite Bonded Joints *Fibre Science and Technology* 17 1982: pp. 77–90.
25. **Yadagiri, S., Reddy, C. P., Reddy, T. S.** Viscoelastic Analysis of Adhesively Bonded Joints *Composite & Structure* 27 1987: pp. 445–454.
26. **Lin, C. C., Lin, Y. S.** Improved Theoretical Solutions for Adhesive Lap Joints *International Journal of Solid and Structures* 30 (12) 1993: pp. 1679–1692.
27. **Reddy, J. N., Roy, S.** Nonlinear Analysis of Adhesively Bonded Joints *International Journal of Non-Linear Mechanics* 23 1988: pp. 97–112.  
[http://dx.doi.org/10.1016/0020-7462\(88\)90017-0](http://dx.doi.org/10.1016/0020-7462(88)90017-0)
28. **Roy, S., Reddy, J. N.** Finite-element Models of Viscoelasticity and Diffusion in Adhesively Bonded Joints *International Journal for Numerical Methods in Engineering* 26 (11) 1988: pp. 2531–2546.
29. **Tsai, M. Y., Morton, J.** Three-dimensional Deformation in A Single-lap Joint *Journal of Strain Analysis for Engineering Design* 29 (1) 1994: pp. 137–145.  
<http://dx.doi.org/10.1243/03093247V292137>
30. **Zhao, L.-B., Qin, T.-L., Shenoi, R.-A., Zhang, J.-Y., Liang, X.-Z., Huang, H.** Strength Prediction of Composite II Joint Under Tensile Load *Journal of Composite Materials* 44 (23) 2010: pp. 2759–2778.  
<http://dx.doi.org/10.1177/0021998310369593>
31. **Zhao, L.-B., Zhang, X.-X., Zhang, J.-Y., Huang, H., Liang, X.-Z.** Failure Analysis of Woven Composite II Joint Under Bending Load *Advanced Science Letters* 4 (8–10) 2011: pp. 2752–2758.
32. **Fu, Y., Zhang, J.-Y., Zhao, L.-B.** Strength Prediction of Composite II Joint under Bending Load and Study of Geometric and Material Variations Effects *Journal of Composite Materials* 47 (8) 2013: pp. 1029–1038.
33. **Zhang, J.-Y., Zhao, L.-B., Qin, T.-L., Fei, B. J.** Influence of II Overlaminates on the Mechanical Behavior of All-composite Adhesively Bonded II Joints *Journal of Reinforced Plastics and Composites* 33 2014: pp. 923–934.  
<http://dx.doi.org/10.1177/0731684414522331>
34. **Zhao, L.-B., Qin, T.-L., Yuli Chen, Y.-L., Zhang, J.-Y.** Three Dimensional Progressive Damage Models for Cohesively Bonded Composite II Joint *Journal of Composite Materials* 48 (6) 2014: pp. 702–721.  
<http://dx.doi.org/10.1177/0021998313477169>
35. **Zhao, L.-B., Gong, Y., Qin, T.-L., Mehmood, S., Zhang, J.-Y.** Failure Prediction of Out-of-plane Woven Composite Joints Using Cohesive Element *Composite Structure* 106 2013: pp. 407–416.
36. **Zhou, D.-W., Louca, L.-A., Saunders, M.** Numerical Simulation of Sandwich T-joints Under Dynamic Loading *Composites: Part B* 39 2008: pp. 973–985.  
<http://dx.doi.org/10.1016/j.compositesb.2007.12.002>
37. **Goncalves, J.-P.-M., de Moura, M.-F.-S.-F., de Castro, P.-M.-S.-T.** A Three-dimensional Finite Element Model for Stress Analysis of Adhesive Joints *International Journal of Adhesion and Adhesive* 22 2002: pp. 357–365.
38. **Bogdanovich, A.-E., Kizhakketharab, I.** Three-dimensional Finite Element Analysis of Double-lap Composite Adhesive Bonded Joint Using Submodeling Approach *Composites: Part B* 30 1999: pp. 4537–551.
39. **Marcadona, V., Nadota, Y., Royb, A., Gacougnolle, J.L.** Fatigue Behaviour of T-joints for Marine Applications *International Journal of Adhesion and Adhesive* 26 2006: pp. 481–489.  
<http://dx.doi.org/10.1016/j.ijadhadh.2005.07.002>
40. **Panigraha, S.-K., Pradhan, B.** Through-the-width Delamination Damage Propagation Characteristics in Single-lap Laminated FRP Composite Joints *International Journal of Adhesion and Adhesive* 29 2009: pp. 114–124.
41. **Tsai, M. Y., Morton, J.** The Effect of a Spew Fillet on Adhesive Stress Distributions in Laminated Composite Single-lap Joints *Composite Structures* 32 (1) 1995: pp. 123–131.
42. **Diaz, J., Romera, L., Hernandez, S., Baldomir, A.** Benchmarking of Three Dimensional Finite Element Models of CFRP Single-lap Bonded Joints *International Journal of Adhesion and Adhesive* 30 2010: pp. 178–189.
43. **Kollar, L. P., Springer, G. S.** Mechanics of Composite Structures. Cambridge University Press, 2009: pp. 11–38.